Optical and Quantum Electronics 7 (1975) 197–209

Raman and fluorescence lidar measurements of aircraft engine emissions

D. A. LEONARD
Avco Everett Research Laboratory Inc, Everett, Massachusetts 02149

Received 5 November 1974

Laser induced Raman and fluorescent measurements were made in the exhaust of a gas turbine engine with a new field portable instrument devised specifically for gas turbine exhaust measurements. The gas turbine exhaust was analyzed by conventional instruments for CO, CO_2, NO, NO_x, total hydrocarbons, smoke and temperature, and these data were used as a 'calibration' standard for the evaluation of the laser Raman instrument. Results thus far indicate good correlations for CO_2, O_2, smoke, hydrocarbons and temperature. The instrument was not sensitive enough for NO detection but the data analysis indicates that 100 ppm may be detectable with instrument improvements. CO analysis was not attempted, but it is expected that CO could be detected with further research. NO_2 (or NO_x) was not attempted because theoretical and experimental laboratory analysis indicated severe interference with CO_2. The conclusion was that laser Raman shows a good potential for aircraft gas turbine emission analysis.

1. Introduction

The purpose of this paper is to report experimental laser induced Raman and fluorescence measurements of combustion exhausts. The work was motivated by a desire to develop an optical means of performing gas analysis of combustion products of aircraft turbine engines in the field which does not require the placement of a physical probe in the exhaust volume and which could be fully automated.

The optical method selected for investigation is the classical Raman scattering technique [1]. This type of optical interaction is well understood both theoretically and experimentally, and can produce extremely accurate and absolute measurements of the mole fraction concentration of the molecular species in a gas mixture. Perhaps the best known field application of the Raman method has been its use by meteorologists to remotely determine, from the ground, water vapour profiles as a function of altitude in the atmosphere [2, 3].

No attempt was made during this investigation to study or compare the various other optical methods that are available for use in addition to the classical Raman technique. Certainly there are both scattering and absorption techniques using finely tuned lasers and resonant interactions that are currently being researched and developed and which may be as useful or more useful than the classical Raman process.

The experimental apparatus that was utilized has been previously described in detail elsewhere [4, 5]. The laser transmitter was a pulsed nitrogen laser operating at 337 nm at a one-half watt average power level with 100 kW pulses at 500 pulses s^{-1}. The receiver consisted of a fully computer controlled double 1 m spectrometer with combined photon counting and synchronous detection.

The aircraft combustor utilized in this work was an Avco Lycoming T-53 Gas Turbine Combustor, the emissions from which had previously been thoroughly investigated by conventional methods [6]. In addition, the emissions from a small piston engine and a simulated exhaust gas generator were also

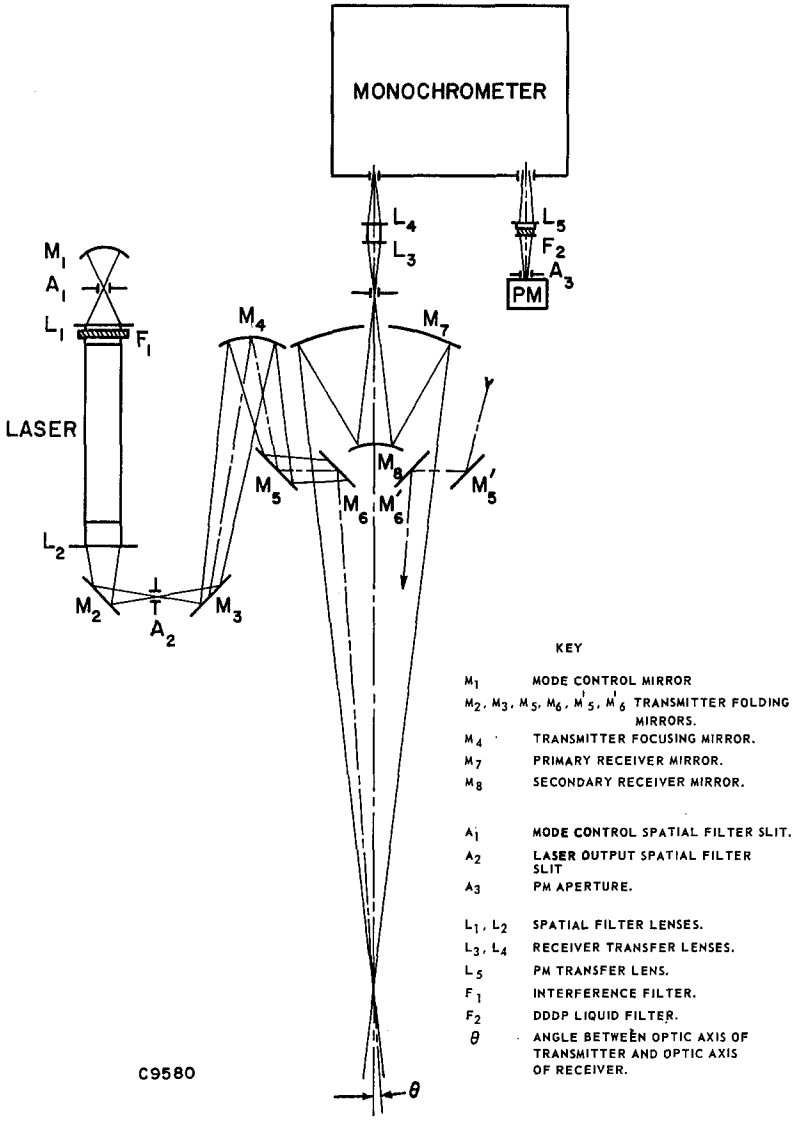

Figure 1 Schematic of transmitter and receiver.

utilized for purposes of instrument development and calibration.

Raman data were obtained which could be used to accurately measure the mole fractions of the major species in the flow, i.e. N_2, O_2, CO_2 and H_2O over the entire range of engine operating conditions from idle to full power. These Raman measurements were compared with the expected values of the specie concentrations as calculated from the measured fuel/air ratio at the various operating conditions.

A problem area that was discovered during the investigation was the presence of a relatively high level of laser induced fluorescence which acted as a noise source and which prevented the detection via the Raman method of low level species such as NO which is typically present at 100 ppm levels. The intensity of the fluorescence could be correlated, however, with the concentration of unburned hydrocarbons as independently measured by conventional means using a gas sampling probe technique.

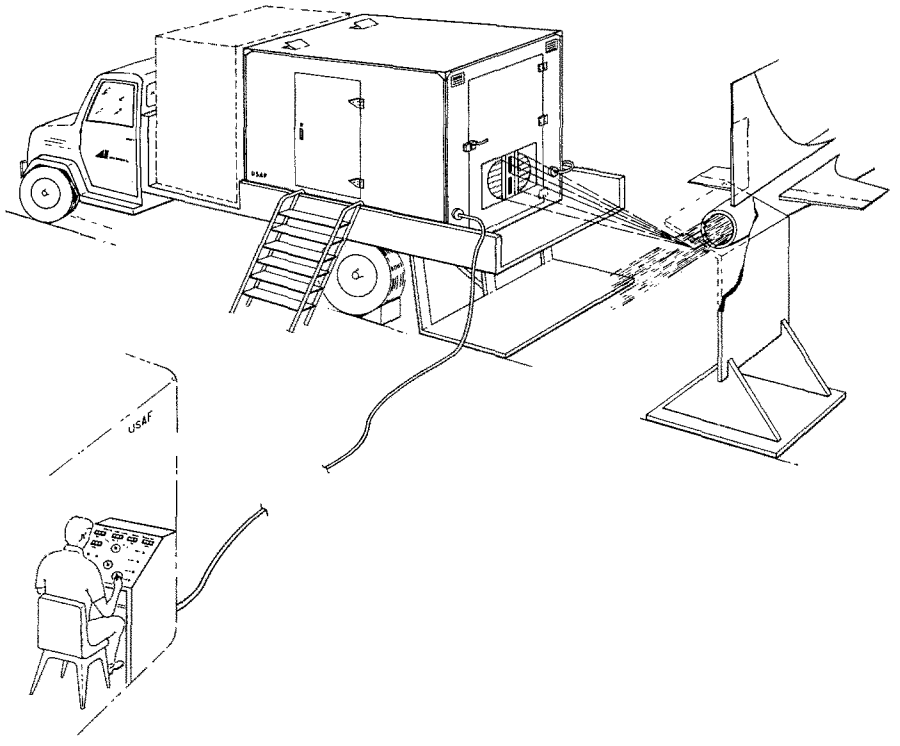

Figure 2 Schematic of laser Raman field measurement system.

Measurements were also made of the radial profiles of the exhaust temperature, using the Raman N_2-density method.

2. Experimental apparatus

As noted above, the experimental apparatus that was utilized in this investigation has been previously described in detail elsewhere [4, 5]. However, certain special features of the apparatus that are critical to the aircraft turbine engine exhaust measurements and their correct interpretation have not previously been emphasized and will be discussed in the following.

The primary function of the transmitter and receiver optics is to transmit the laser beam to the desired volume of the exhaust gases to be analyzed and then provide for efficient collection of the Raman scattered photons from that same measurement volume. In addition, it is equally important that scattering caused by the laser beam from gas located outside the desired measurement volume be just as efficiently rejected. In other words, the laser beam and the field of view of the collector should have a sharply peaked overlap in the measurement volume of interest. The details of this optical engineering design trade-off have been previously reported by Munroe [7].

The general schematic arrangement of the transmitter and receiver optics is shown in Fig. 1. Basically, the laser spatial filter slits are imaged by the transmitter onto the exhaust volume which is to be analyzed, and which is then re-imaged by the collector mirror onto the entrance slit of the spectrometer.

The aspect ratio of the laser spatial filters is matched to the rectangular entrance slit of the spectrometer. This technique of using coherent amplification in the laser to produce a beam of optimal specification improves the overall conversion efficiency of available laser energy to detected Raman signal. The laser Raman transmitter and receiver system was installed in a mobile van so that field measurements of aircraft turbine engine emissions could be performed. Fig. 2 is a schematic of the field measurement system. The measurement volume at the common transmitter and receiver focus is positioned approximately 2 m from the rear of the van. The measurement volume is approxi-

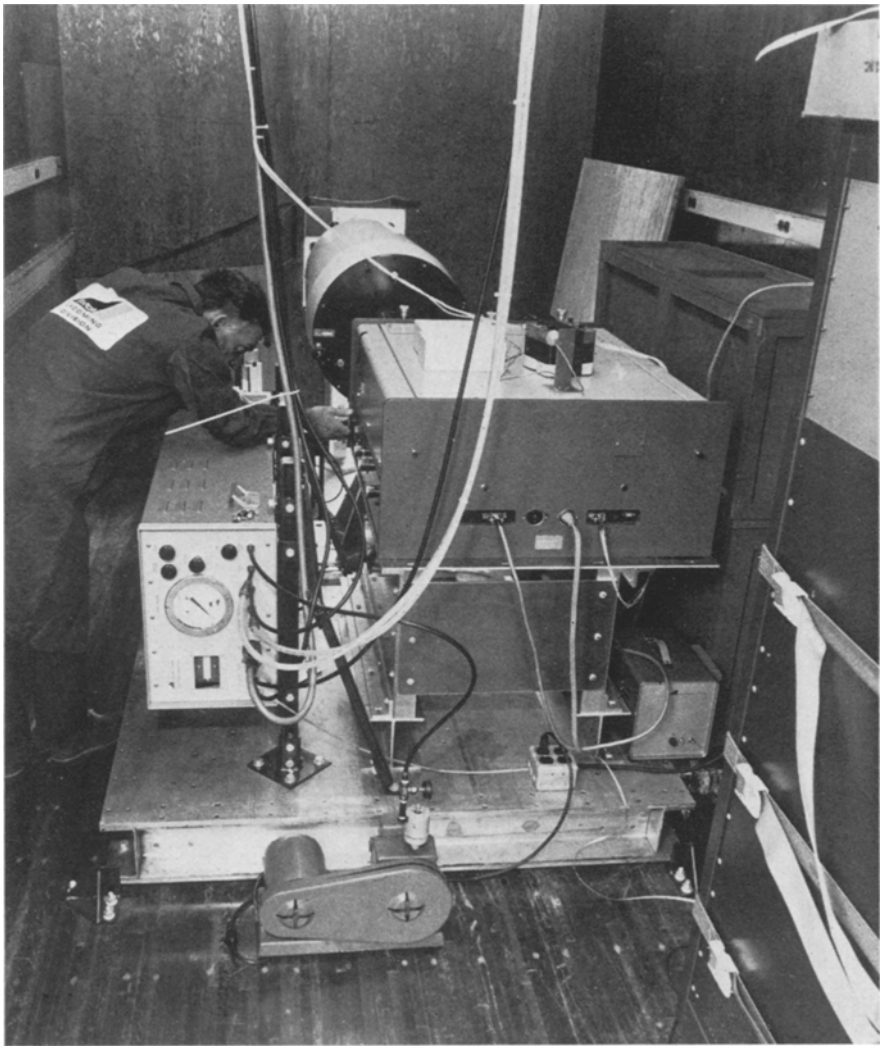

Figure 3 Photograph of optical transmitter and receiver system mounted in portable van.

mately a rectangular slab, of dimensions 0.1 × 1 × 1 cm with the small dimension of the slab oriented in the direction of the flow, so as to average over as many streamlines as possible.

The measurement van is shown in Fig. 3. Fig. 3 shows the optical transmitter and receiver system mounted on the rigid aluminium pallet and as installed within the mobile van. The rectangular box-like structure with the pressure gauge mounted on the end plate is the pulsed nitrogen laser. The operator is shown adjusting the wavelength setting of the double spectrometer. The round barrel-like structure behind and slightly to the left of centre of the spectrometer is the Cassegrain collection optics. The pallet is isolated from the floor of the van by means of shock mounts.

Other aspects of the experimental apparatus which have been critical to the overall success of the measurement system are the data acquisition and system control techniques. The most efficient photoelectric detection scheme at low light levels is actual quantum counting. However, the system had to be built to handle a large dynamic range, i.e., to include both the low level measurement of pollutant species such as NO in

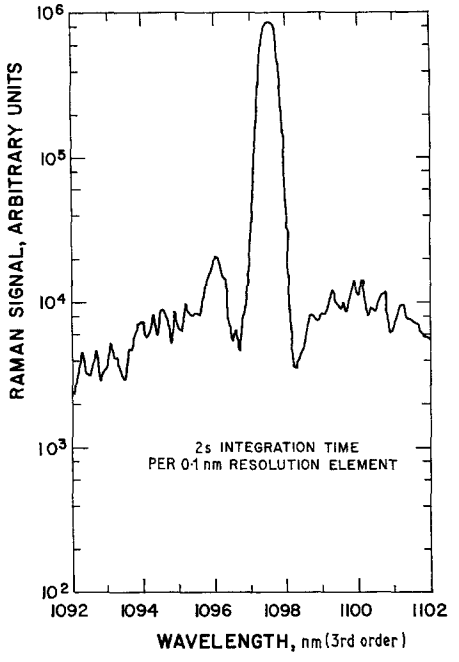

Figure 4 Ambient air nitrogen vibrational Raman line at 2330 cm^{-1}.

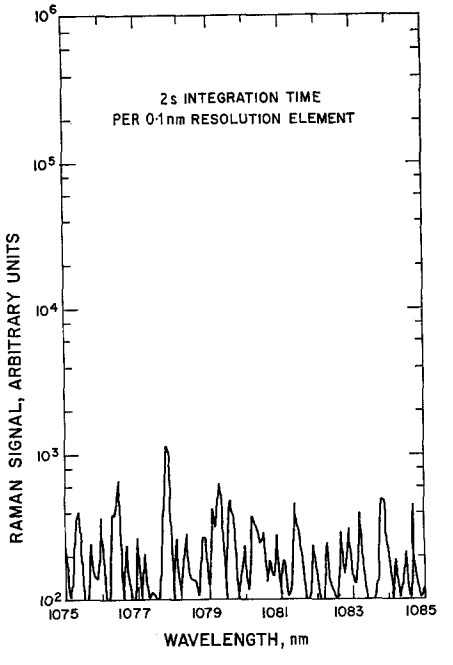

Figure 5 Spectral scan at 1876 cm^{-1} showing system noise level.

the 10 to 100 ppm range as well as the simultaneous sequential measurement of N_2 for calibration purposes at a concentration of 10^4 to 10^5 times greater, and in the same data channel.

Realtime data processing with a Data General Nova programmable digital processor provides for actual single quantum counting at the low light levels and for charge encoding at the higher light levels to allow for many photoelectrons being produced in one laser pulse gate time. Other features of the data processing include automatic wavelength calibration of the spectrometer using the N_2 Raman line position, automatic programmable wavelength scanning and detection time gate scanning, ambient light background subtraction on a pulse to pulse basis, fluorescence subtraction using both the wavelength and time domains, and both temperature measurement and temperature corrections applied to the spectra to obtain correct specie concentrations as a function of temperature.

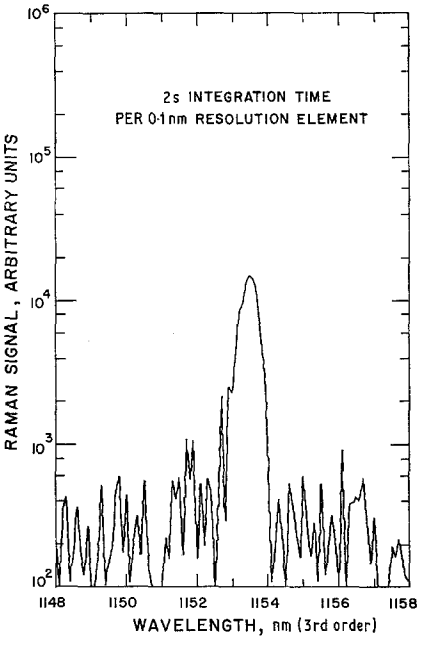

Figure 6 Atmospheric water vapour vibrational Raman line at 3652 cm^{-1}.

3. Experimental results

Initial tests were conducted to prove and demonstrate the basic performance of the laser Raman field unit using normal atmospheric air as a test gas. Figs. 4, 5 and 6 show spectra obtained in the spectral regions that correspond to vibrational Raman transitions in nitrogen, nitric oxide and

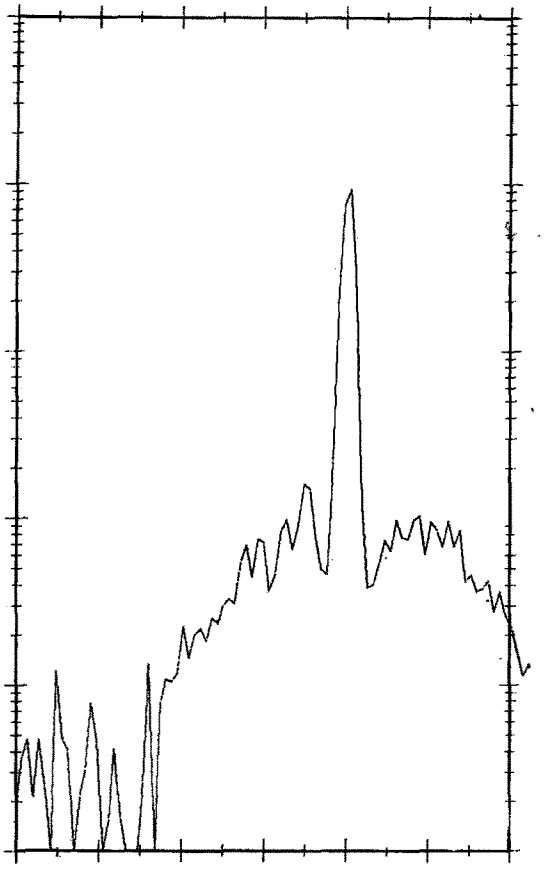

Figure 7 Ambient air nitrogen vibrational Raman line at 2330 cm^{-1}, with $\Delta J = \pm 2$ rotational sidebands.

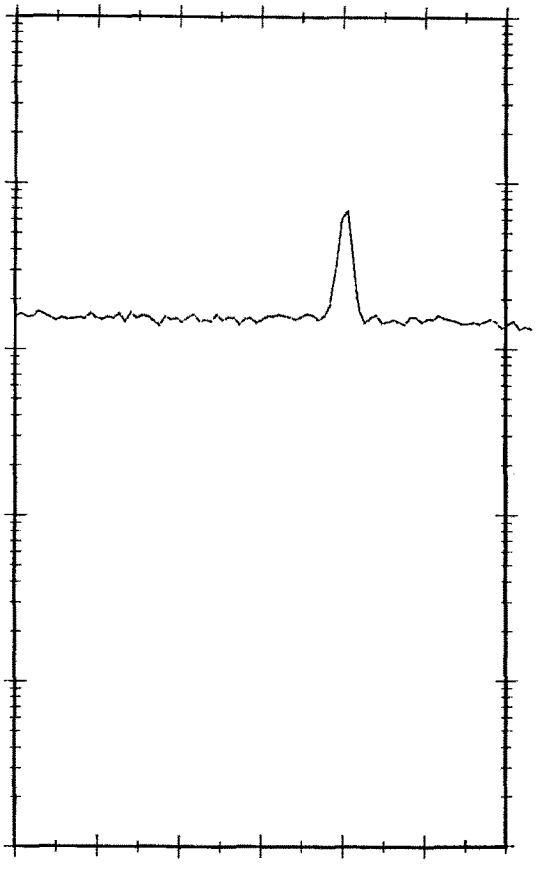

Figure 8 Nitrogen vibrational Raman line at 2330 cm^{-1} with broad band hydrocarbon fluorescence in combustor exhaust.

water vapour, at 2330, 1876 and 3652 cm^{-1} respectively.

As shown, a dynamic range of about four orders of magnitude (i.e., 10 000) is available between the signal from N_2 in Fig. 4 and the noise level at the NO concentration of about 1% of the atmospheric nitrogen signal in Fig. 4. It should be noted that the wavelength scale on these Figs. is 3 times the actual wavelength of the spectra since the grating was used in the third order when this data was taken.

Following these preliminary atmospheric ambient air tests, the van containing the laser Raman gas analyzer was moved to the AVCO Lycoming engineering test facility and laser Raman tests were conducted with a Lycoming simulated exhaust stream generator and on actual T-53 Lycoming gas turbine engine combustor. Simultaneous analytical probe measurements were made of the gas conditions in the streamlines passing through the laser scattering volume.

With the laser Raman van in place at the Lycoming test site, the Raman spectrum in Fig. 7 was obtained before the exhaust stream generator was operated. This spectrum shows, on a semi-logarithmic scale, the usual atmospheric nitrogen vibrational line with its rotational side-bands at about 1% of the peak value and an ambient noise level at about the 0.01% level compared to the nitrogen peak. The spectrum in Fig. 7 thus showed that the laser Raman gas analyzer system was working in accordance with its design.

When the exhaust stream generator was operated under simulated 'idle' conditions and produced several hundred ppm of hydrocarbon emissions, spectra such as shown in Fig. 8 were

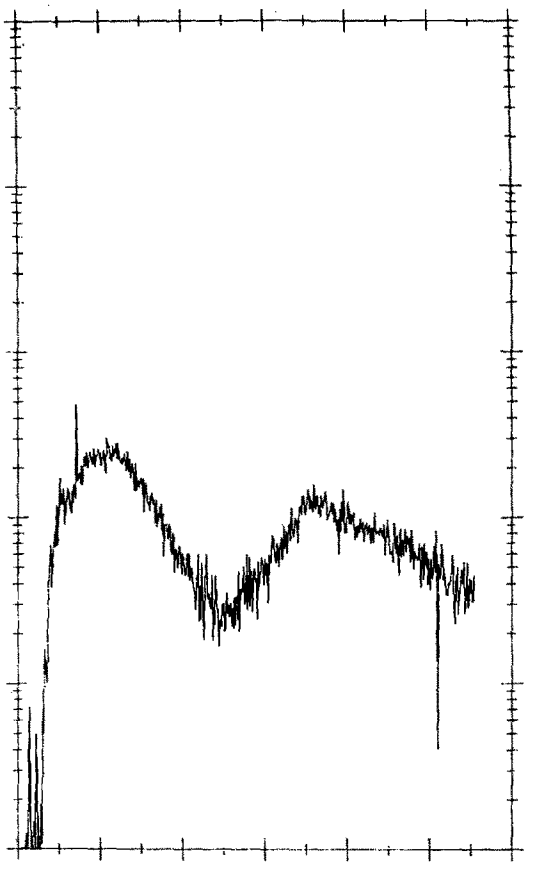

Figure 9 Scan of hydrocarbon fluorescence spectrum from 300 to 600 nm.

obtained. This figure shows a scan of the same spectral region as previously shown in Fig. 7 which includes the nitrogen Raman line. What is most apparent in Fig. 8 is that with the high concentration of hydrocarbon emissions present, a laser induced continuum level is produced which is the same order of magnitude as the nitrogen Raman peak.

A much broader spectral scan, from 300 to 600 nm with the same exhaust condition is shown in Fig. 9. This figure shows that the continuum level is present from essentially the laser excitation wavelength at 337 to beyond 500 nm. Such a broad emission spectrum would be typical of a mixture of unsaturated hydrocarbons which are excited by a 337 nm source.

The dip in the spectrum of Fig. 9 at about 450 nm is an artifact caused by the spectral response of the receiver – primarily due to the properties of the gratings used in the SPEX double spectro-

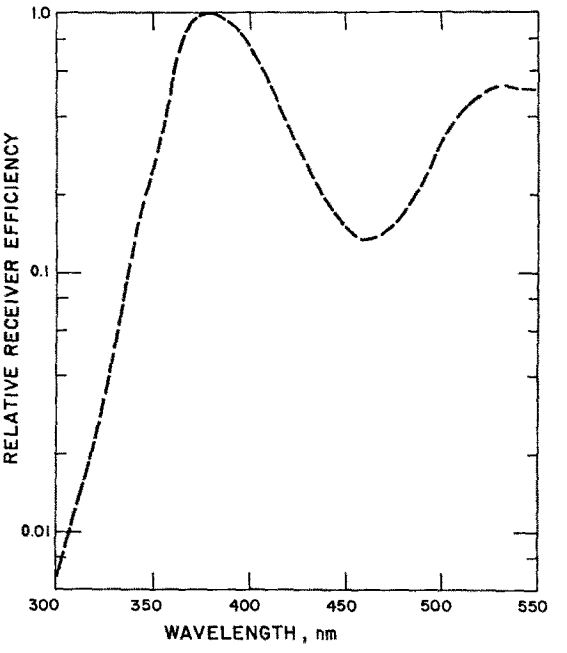

Figure 10 Receiver response function.

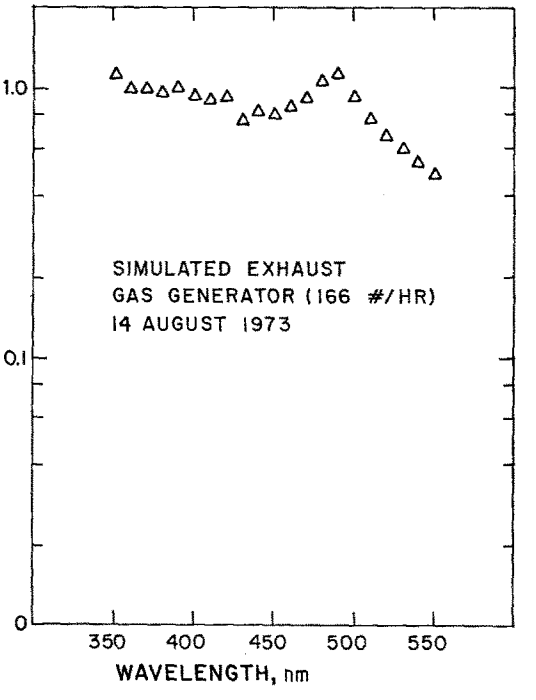

Figure 11 Normalized fluorescence spectrum – simulated exhaust gas generator.

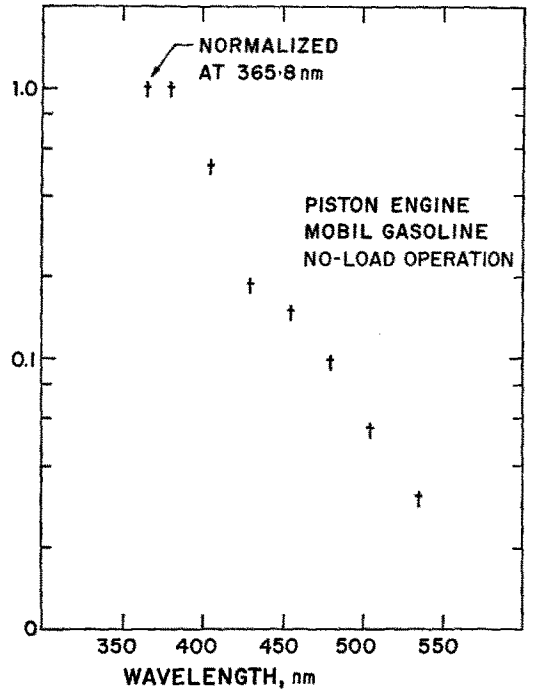

Figure 12 Normalized fluorescence spectrum – piston engine.

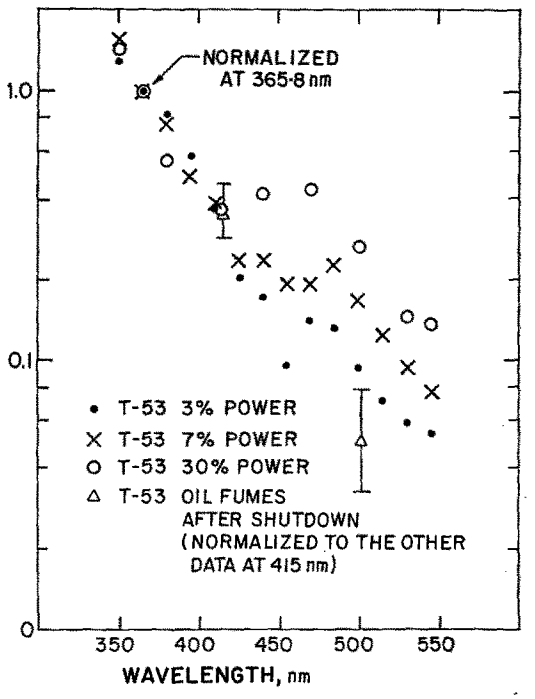

Figure 13 Normalized fluorescence spectrum – lycoming T53 gas turbine engine.

meter. Fig. 10 shows the relative spectral response of the receiver as determined by means of a NBS Standard Lamp calibration procedure and clearly indicates a similar dip at 450 nm. When the hydrocarbon fluorescence spectrum of Fig. 9 is normalized with respect to the receiver response function in Fig. 10, the actual hydrocarbon fluorescence is seen to be essentially flat in the 400 to 500 nm spectral region as shown in Fig. 11.

Similar measurements were made of the 337 nm laser induced fluorescence properties of the exhaust of the Lycoming T-53 gas turbine engine and also the exhaust of a small piston. The normalized fluorescence spectra from these engines are shown in Figs. 12 and 13. A reasonable correlation can be made between the piston engine spectra and the T-53 spectra at idle conditions and with the fluorescence spectra of the engine oil as measured in the field and also in the laboratory tests [8]. The spectra produced at the higher power settings with the T-53 is beginning to resemble the simulated combustor spectra where presumably no engine oil was present.

The absolute level of the fluorescence spectra relative to the N_2 Raman peak at the wavelength of the N_2 Raman line is 0.3, 0.05, 0.01 and 0.01 for T-53 engine power settings of 7, 30, 60 and 100% of full power respectively. Thus a fluorescence level of this magnitude will be a serious interference and a noise source for Raman measurements of species concentration at the 1% level and lower.

A possibility for enhancement of the Raman spectra in the presence of a fluorescence noise background is the fact that the Raman spectra is prompt, i.e. follows the laser pulse shape, whereas the fluorescence spectra might be expected to have a finite lifetime, significantly longer than the 10 ns nitrogen laser pulse duration. Measurements were made of the lifetime of the fluorescence in the piston engine exhaust and in the T-53 exhaust. A 5 ns wide detection gate was scanned in time in 2.5 ns increments over a 100 ns total range of time which included the coincidence condition, i.e., the time at which the Raman lines are observed. Typical such data are shown in Fig. 14. The fluorescence decay time is determined by the

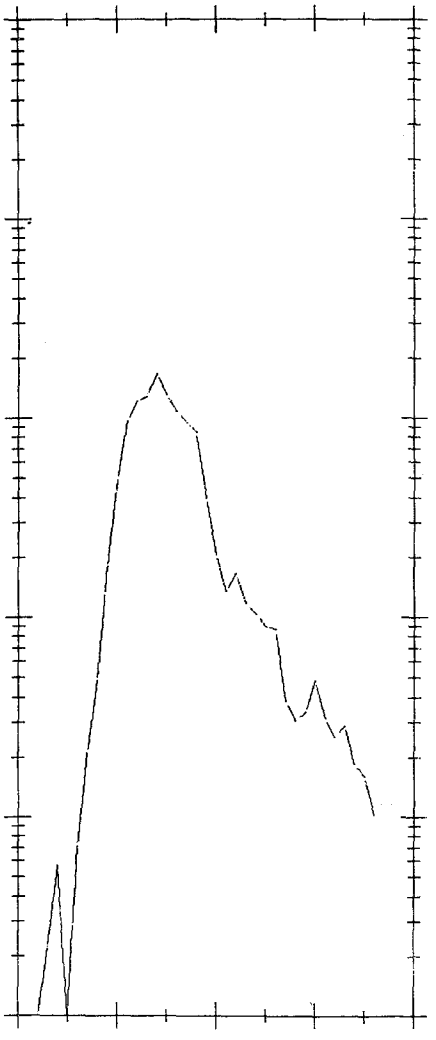

Figure 14 Typical data showing fluorescence decay time measurements.

slope of the trailing edge of such data.

A plot of the measured fluorescence decay times as a function of wavelength is shown in Fig. 15. The observed decay time increases with wavelength from about 4 ns at 360 nm to about 10 or 12 ns at 500 nm. The laser pulse decay time of 3 ns should be subtracted from the observed fluorescence decay times to obtain the true values. A detailed analysis has been made of the improvement in S/N that can be achieved by using shorter laser pulse durations and leading edge detection and it is planned to report this work elsewhere in the future [9].

Very accurate Raman measurements were

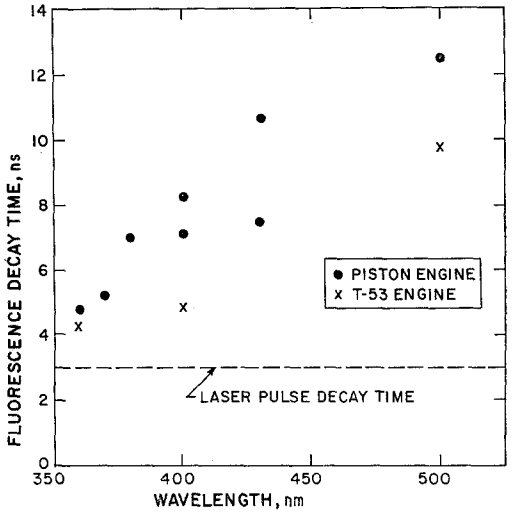

Figure 15 Fluorescence decay time versus wavelength.

made of the O_2 and CO_2 concentrations in the T-53 engine exhaust and these measurements show excellent agreement when compared with the expected values of the concentration of these species on the basis of the measured fuel/air ratio of the actual operating engine.

Typical data of the O_2 vibrational Raman line in the hot exhaust gases is shown in Fig. 16. This data corresponds to an engine power setting of 30%. The dip in the data trace at the right side shows the results of temporarily turning off the laser during the scan, indicating that the background level is entirely a laser induced signal. The value of the O_2 signal is obtained by subtracting the average fluorescence level from the observed signal at the O_2 Raman line position. In a similar manner, the N_2 Raman signal for the same engine condition is obtained after suitable corrections for the fluorescence level in that spectral region. The ratio of the corrected O_2 to N_2 Raman signals can then be used to obtain the O_2/N_2 mole ratio. The system was calibrated in the field for effective cross-section and system transfer function by using the O_2/N_2 ratio obtained from ambient air and assuming that air is 21% O_2 and 79% N_2 on a mole basis.

The results of the oxygen measurements are shown in Fig. 17 where the O_2/N_2 mole ratio as obtained from the Raman measurements is plotted as a function of the O_2/N_2 mol ratio as calculated from the fuel/air (F/A) ratio of the

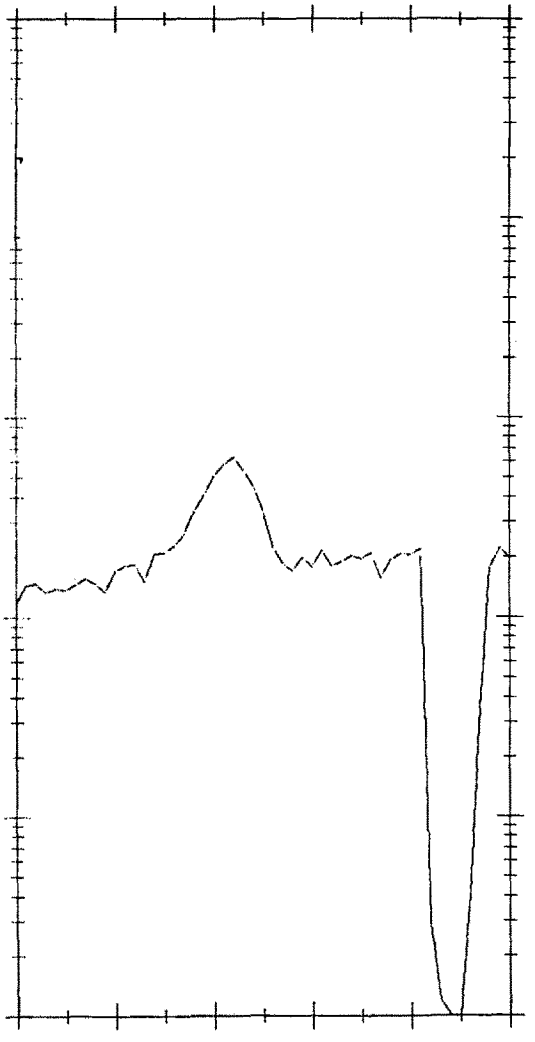

Figure 16 Oxygen vibrational Raman line at 1556 cm^{-1} with fluorescence background.

actual operating Engine. Perfect agreement would cause the data to fall on the line connecting zero with the point labelled 'air'. It can be seen that the data fall generally along that line to within the accuracy of the respective measurements. The error bars are mainly due to the shot noise in the Raman signal at the high power conditions and are dominated by the fluctuations in the higher fluorescence levels at the lower power conditions. A minor temperature correction due to the difference in the vibrational Boltzmann factor between O_2 and N_2 should be applied to such data if higher precision is required.

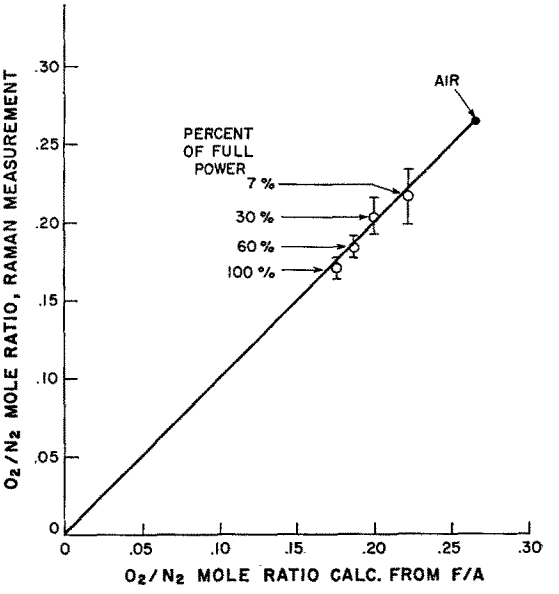

Figure 17 O_2/N_2 mol ratio for T-53 engine. Raman measurement versus calculated value.

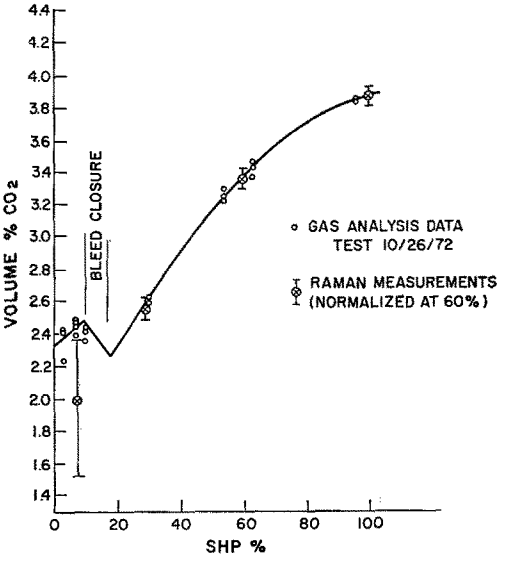

Figure 18 Vol.% CO_2 versus % shaft horsepower (SHP).

Similar Raman measurements were made of the CO_2 concentration in the T-53 turbine engine exhaust. The results of these measurements are displayed in Fig. 18 which shows the vol. % CO_2 as a function of the percent shaft horse power (SHP) of the engine. The Raman

data was normalized to the gas analysis data at the 60% power point. As with O_2, the Raman data and the gas analysis data are seen to be in agreement to within the accuracy of the respective measurements.

Water vapour Raman data was also obtained from the T-53 engine exhaust under all operating conditions. Uncertainty in the water vapour Raman cross-section as a function of temperature has precluded the use of the water vapour Raman data to obtain water vapour concentrations.

A recent attempt was made to detect nitric oxide (NO) in the T-53 exhaust using the 1876 cm^{-1} vibrational Raman transition. The T-53 engine typically produces 100 ppm of NO when operating at full power. Since the fluorescence level in the T-53 at full power was about 100 times greater than the expected signal from NO, the required integration times for detection were longer than the test time available with the T-53. The data obtained and shown in Fig. 19 do

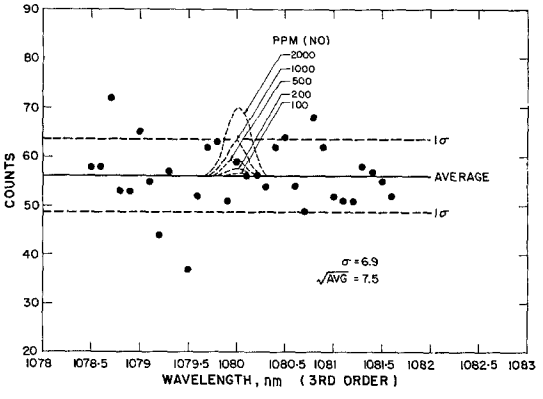

Figure 19 Raman/fluorescence data obtained on the T-53 exhaust in the NO spectral region.

illustrate the problem, however. This figure shows a spectral scan through the wavelength region of the NO Raman line. The average value of the fluorescence level is approximately 56 counts for each measurement time period of 90 s. During the same time period the expected NO Raman signal for 100 ppm will be 0.7 counts. Since this is well within the standard deviation of the fluorescence level (6.9 counts), the NO was not detected by the measurement. As shown on the figure a level of 2000 ppm of NO would have been detected, since that would have satisfied the

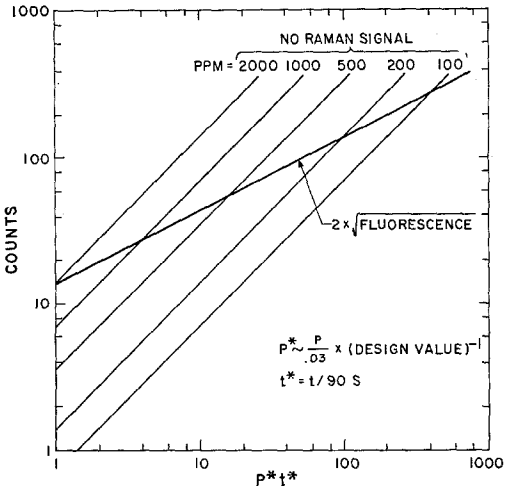

Figure 20 Raman counts from NO as a function of the normalized laser power × integration time product with the fluorescence interference threshold shown.

detection criteria that the mean of the NO + fluorescence signal and the mean of the fluorescence signal would be separated by two standard deviations.

Assuming a constant level of fluorescence, the chart of Fig. 20 shows the scaling of the measurement with NO concentration and a normalized laser power and integration time product. The intersections of the line labelled $2 \times \sqrt{\text{Fluorescence}}$ with the various NO Raman signal lines indicate operating points at which the Raman signal from NO is twice the standard deviation of the fluorescence level. The measurement described by Fig. 19 falls at the point $P^*t^* = 1$ where P was 3% of the design value (due primarily to optical transmission loss) and t was 90 s. The use of the chart may be illustrated by the following example. A value of $P^*t^* = 100$ would be required to detect NO at 200 ppm. This could be accomplished by increasing P to the design value (i.e. cleaning the optics) and integrating for 4.5 min.

The temperature of the T-53 exhaust was measured by means of the N_2 Raman density method whereby the temperature is assumed to be inversely proportional to the density of nitrogen, with a constant static pressure [10]. If the dynamic pressure is a significant portion of the total pressure, i.e., in a high velocity flow, then a correction for this must be made to the data.

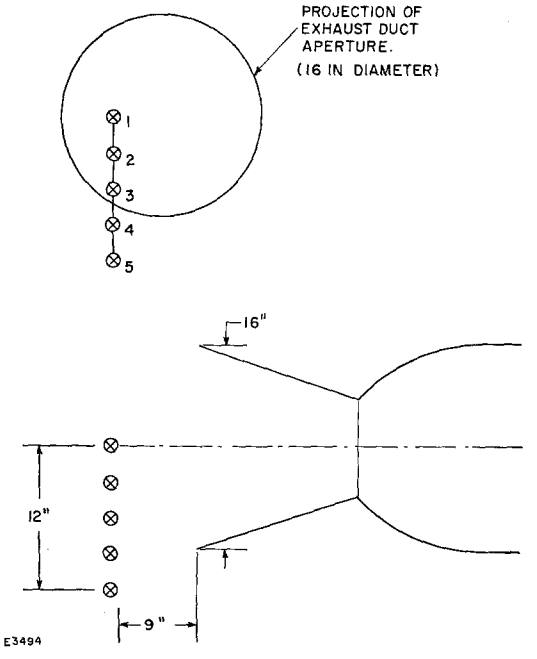

Figure 21 Geometry of N_2 density method temperature profile.

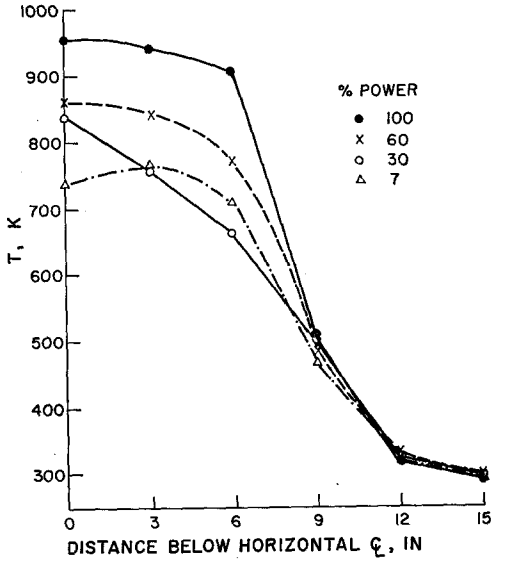

Figure 22 Temperature profiles T-53 engine exhaust using Raman density method.

The density of nitrogen was measured at six points in the exhaust stream of the T-53 for each of the four operating conditions. The geometry of the profile and the position of the measurements points in the exhaust stream is shown in Fig. 21. The temperature and density of the ambient air was used as a scale factor to obtain the temperature profiles shown in Fig. 22. Thermocouple measurements in the exhaust stream gave 725 K for the 7% power point and 890 K for the 100% power point. The lower power points are in reasonable agreement. The higher power Raman data is somewhat higher than the thermocouple, but a thermocouple radiation correction is probably necessary.

4. Conclusions

The classical laser Raman technique has been shown experimentally to be a viable optical method for the analysis of aircraft engine exhausts under field conditions.

Accurate measurements have been obtained for the concentrations of O_2 and CO_2 which are in excellent agreement with both conventional probe measurements and the concentration values calculated from the measured engine fuel/air ratio.

The species present at lower concentrations such as NO at 100 ppm have not been detected in actual field measurements due to interference with a low level hydrocarbon fluorescence background. However, extrapolations from the data obtained indicate that a refurbished optical system operating at its nominal design throughput could detect NO at 100 ppm in less than 5 min integration time.

Temperature profiles of the engine exhaust were also obtained from the Raman spectra which are in good agreement with thermocouple measurements.

Acknowledgement

This work was supported by the Air Force Aero Propulsion Laboratory, United States Air Force, Wright Patterson Air Force Base, Ohio under Contract F33615-71-C-1875.

The author acknowledges valuable conversations with M. Roquemore, WPAFB and F. N. Hodgson, Monsanto Research Corporation, Dayton, Ohio.

References

1. C. V. RAMAN and K. S. KRISHNAN, *Nature* **121** (1928) 501-502.
2. S. MELFI, J. LAWRENCE and M. MCCORMICK, *Appl. Phys. Lett.* **15** (1969) 295-297.

3. R. G. STRAUCH, V. E. DERR and R. E. CAPP, *Remote Sensing of Environment* **2** (1972) 101.
4. D. A. LEONARD, 'Development of A Laser Raman Aircraft Turbine Engine Exhaust Emissions Measurement System, Technical Report,' Avco Everett Research Laboratory, Research Note 914.
5. G. E. BRESOWAR and D. A. LEONARD, AIAA Paper No. 73-1276, presented at the AIAA/SAE 9th Propulsion Conference, November 1973.
6. P. M. RUBINS and B. W. DOYLE, USAAMRDL Technical Report 73-47, 'T53 and T55 Gas Turbine Combustor and Engine Exhaust Emission Measurements,' U.S. Army Air Mobility Research and Development Laboratory, Fort Eustis, Virginia.
7. J. L. MUNROE, *Optic. Eng.* **13** (1974) 79.
8. F. N. HODGSON, Monsanto Research Corporation, Dayton, Ohio, private communication.
9. M. ROQUEMORE, WPAFB, private communication.
10. R. G. STRAUCH, V. E. DERR and R. E. CAPP, *Appl. Optic.* **10** (1971) 2665-2669.